



HAL
open science

Catalytic cracking of ethylbenzene as tar surrogate using pyrolysis chars from wastes

Maxime Hervy, Audrey Villot, Claire Gerente, Doan Pham Minh, Elsa
Weiss-Hortala, Ange Nzihou, Laurence Le Coq

► **To cite this version:**

Maxime Hervy, Audrey Villot, Claire Gerente, Doan Pham Minh, Elsa Weiss-Hortala, et al.. Catalytic cracking of ethylbenzene as tar surrogate using pyrolysis chars from wastes. *Biomass and Bioenergy*, 2018, 117, pp.86-95. 10.1016/j.biombioe.2018.07.020 . hal-01867484

HAL Id: hal-01867484

<https://imt-mines-albi.hal.science/hal-01867484>

Submitted on 6 Nov 2018

HAL is a multi-disciplinary open access archive for the deposit and dissemination of scientific research documents, whether they are published or not. The documents may come from teaching and research institutions in France or abroad, or from public or private research centers.

L'archive ouverte pluridisciplinaire **HAL**, est destinée au dépôt et à la diffusion de documents scientifiques de niveau recherche, publiés ou non, émanant des établissements d'enseignement et de recherche français ou étrangers, des laboratoires publics ou privés.

Catalytic cracking of ethylbenzene as tar surrogate using pyrolysis chars from wastes

Maxime Hervy^{a,b,*}, Audrey Villot^a, Claire Gérente^a, Doan Pham Minh^b, Elsa Weiss-Hortala^b, Ange Nzihou^b, Laurence Le Coq^a

^a IMT Atlantique, GEPEA UMR CNRS 6144, 4 Rue A. Kastler, CS 20722, Nantes Cedex 03, 44307, France

^b Université de Toulouse, Mines Albi, CNRS, Centre RAPSODEE, Campus Jarlard, Route de Teillet, F.81013, Albi Cedex09, France

ABSTRACT

This paper aims at studying the catalytic activity of waste-derived chars for the reforming of a tar compound (ethylbenzene), and to identify the relationships between the modification process, the physicochemical properties and their resulting catalytic behaviour. Two chars were produced by pyrolysis: (1) used wood pallets (UWP), and (2) a mixture of food waste (FW) and coagulation-flocculation sludge (CFS) from wastewater treatment plant. Two chemical-free modification processes were separately applied to the pyrolysis chars: a gas phase oxygenation at 280 °C, or a steam activation at 850 °C. At 650 °C, the ethylbenzene conversion due to thermal cracking was significantly increased by the catalytic activity of the chars (from 37.2 up to 85.8%). Ethylbenzene was decomposed into six molecules: hydrogen, carbon dioxide, ethylene, benzene, styrene, and toluene. Cracking, oxidative dehydrogenation, and hydrogenolysis reactions were involved in the decomposition mechanism of ethylbenzene. The catalytic efficiency of the char was also discussed based on the energy transferred from tar to syngas during tar cracking reactions. The characterization, performed with SEM, XRD, Raman, XRF, BET and TPD- μ GC, evidenced that the presence of mineral species in the metallic form strongly increased the syngas production and quality by catalysing aromatic-ring opening reactions and Boudouard reaction. The oxidation of mineral species, occurring during the oxygenation process, decreased the char efficiency, while rising S_{BET} increased the syngas production for UWP-based chars. This study demonstrated that waste-based chars were efficient catalysts to convert the lost energy contained in tar into useful syngas, thus increasing simultaneously the syngas yield and quality.

Keywords:

Activated carbon
Catalytic cracking
Pyrolysis
Syngas
Tarreforming

1. Introduction

The pyro-gasification of biomass and waste appears as a promising conversion routes to produce a gaseous energy carrier named syngas, mainly composed of H_2 and CO. The pyro-gasification consists in the reaction between biomass or waste and an oxidizing agent (air, steam, O_2 or CO_2) at elevated temperature (800–1000 °C), and leads to the decomposition of the solid fuel in three fractions: syngas, tar, and a solid residue composed of char and/or ash (depending on the carbon content) [1]. Syngas could be valorised in energy conversion applications (power and heat generation by combustion in gas engines, gas turbines, fuel cells ...), and as precursor in the production of liquid fuel (via the Fischer-Tropsch synthesis) or chemicals [2]. However, it should be purified prior to subsequent uses in order to remove impurities originally contained in solid fuels (*i.e.*: sulphur, chlorine, nitrogen compounds, etc.), particles (inorganic elements, soot ...), and pollutants

generated by incomplete gasification (tar) [3].

The formation of tar is the major issue limiting the development of the pyro-gasification technologies. Indeed, tar can condense at high temperature (350 °C) thus fouling the equipment downstream of the gasifier (pipes, filters, heat exchangers ...), or deactivate the catalysts used in the syngas upgrading process [4]. Tar is a complex mixture of condensable aromatic and oxygenated hydrocarbons having a molecular weight higher than benzene (78 g/mol) [2], and are divided in several classes depending on their properties [5,6]. Light aromatic compounds are the main class of tar generated by the pyro-gasification of biomass. Their concentration can vary between 5 and 200 g/Nm³ of syngas [2], while the standards required for syngas utilization vary between 0.01 and 100 mg/Nm³, depending on the end-use [2,3]. Therefore, tar removal from the syngas is mandatory and several methods have been developed to this end [7–10]: physical treatment (electrostatic precipitation, inertial separation, wet or dry scrubbing),

* Corresponding author. IMT Atlantique, GEPEA UMR CNRS 6144, 4 rue A. Kastler, CS 20722, Nantes Cedex 03, 44307, France.

E-mail address: maxime.hervy@mines-albi.fr (M. Hervy).

Abbreviations

AAEM	Alkali and alkaline earth metallic
UWP	Used Wood Pallets
FW	Food Waste
CFS	Coagulation-Flocculation Sludge
c.UWP	char from UWP
c.FW/CFS	char from a mixture of FW (50 wt%) and CFS (50 wt%)
ox	prefix used to name the oxygenated chars
ac	prefix used to name the steam activated chars
TPD	Thermo-Programmed Desorption
EB	Ethylbenzene
X _{EB}	average ethylbenzene conversion (%)

Sel _i	molar selectivity of the tar cracking product <i>i</i> (mol%)
η _C and η _H	fraction of carbon and hydrogen, respectively, transferred from the ethylbenzene molecule to the vapour cracking products
Prod _{syngas}	volume of syngas produced from the cracking of 100 mol of initial ethylbenzene (NL of syngas produced/100 mol of tar)
LHV _{syngas}	lower heating value of the syngas produced from the cracking of 100 mol of initial ethylbenzene (kJ/mol of syngas produced)
ΔE _{syngas}	energy converted from tar to syngas by the conversion of ethylbenzene in permanent gases (kJ/100 mol of initial ethylbenzene)

plasma cracking, thermal cracking and catalytic cracking. The advantages and disadvantages of these methods were summarized by Shen et al. [11]. The catalytic cracking presents several advantages, such as: high reaction rate, the increase of syngas yield and purity, and the use of moderate temperatures [12–17]. Tar cracking aims at converting tar into permanent gases (such as H₂ and CO), thus simultaneously increasing the syngas yield and quality. This reaction allows to transfer the lost energy contained in the tarry-molecules into useful syngas. For these reasons, catalytic cracking of tar appears as a main issue in the development of pyrogasification processes.

Different types of catalysts have been studied for tar removal, such as calcined rocks (dolomite, magnesite and calcite) [18–20], olivine [21,22], clay minerals [5], zeolites [23], iron oxides [24], fluid catalytic cracking catalysts (FCC) [25], noble metals [26–30], alkaline and alkaline earth metals (AAEM) [31,32], nickel catalysts [33] and chars [34–36]. As summarized by Shen et al. [11], each catalyst presents some pro and cons but metal catalysts (such as alumina or activated carbon supported Fe, Ni and Co) appear as the most efficient [37–39]. However, these catalysts suffer from rapid deactivation by coking [40,41], and elevated production costs. The development of low-cost and eco-friendly catalysts remains a main issue to reduce the cost of the syngas cleaning process.

Chars are co-products of the pyro-gasification process and represent 12 to 30 wt% of the initial biomass [42]. This large amount of solid residues should be valorised. Since the costs associated with the char landfilling compromise the economic sustainability of the pyro-gasification units, the valorisation of chars as catalysts for syngas cleaning appears as an attractive approach. This topic has been increasingly investigated over the past few years. Previous studies reported that four characteristics of the chars determined their activity even if their role remains not clear: the porous structures [43,44], the presence of O-containing groups on the char surface [45–49], the structure of the carbonaceous matrix [50,51], and the active sites formed by the inherent alkaline (*i.e.*: Na, K) and alkaline earth (*i.e.*: Mg, Ca) species (AAEM) distributed in the char matrix [52–54]. In addition, these AAEM species can slow the deactivation rate by coke deposition since they can catalyse the gasification reactions of coke [55]. However, chars from biomass usually have low mineral content, and metal impregnation is necessary to enhance their catalytic activity by increasing active sites [56]. This impregnation increases the production cost and the environmental footprint of the resulting catalyst, thus reducing the benefits of using char as catalyst. On the contrary, chars from waste (such as sludge) can be rich in minerals but suffer from low specific surface area and carbonaceous structure, resulting in a fast deactivation by coke deposition [57].

The improvement of the catalytic activity of waste-based pyrolysis chars by applying low-cost and eco-friendly modification processes has scarcely been explored. In the literature, there is also a lack of study focused on the use of chars for the catalytic cracking of light aromatic hydrocarbon compounds other than toluene. This paper aims at

studying the catalytic cracking of ethylbenzene (C₈H₁₀) as a tar model compound over different types of pyrolysis chars from wastes, and functionalised with low-cost processes. A comprehensive set of characterisations (elemental analysis, XRFs, Raman, XRD, N₂ adsorption-desorption, TPD, SEM-EDX) was used to understand the relationships between the modification process, the physicochemical properties of the chars, and their catalytic activity for ethylbenzene cracking. The selectivity of the ethylbenzene cracking products was investigated in order to identify the reactions involved in the decomposition mechanisms. In order to determine the performance of each char in increasing the syngas production and quality, three parameters were calculated: the volume of syngas produced by tar cracking reaction, the lower heating value (LHV) of the produced syngas, and the energy transferred from tar to syngas during the ethylbenzene decomposition.

2. Materials and methods

2.1. Catalysts production

2.1.1. Pyrolysis treatment

The waste materials used in this study were obtained from cruise ships. However, they are generated in large amount by modern societies: Used Wood Pallets (UWP), Food Waste (FW) and Coagulation-Flocculation Sludge (CFS). UWP was made of softwood, previously employed in the production of pallets for food transportation. Food Waste was composed of a mixture of vegetables and animal wastes. Coagulation-Flocculation Sludge was recovered from a wastewater treatment plant present on board.

The chars were produced by pyrolyzing wastes at 700 °C during 30 min (heating rate of 22 °C/min) in a semi-continuous horizontal screw reactor (internal diameter of 0.167 m and 2 m in length). The details on the experimental procedure were described in a previous papers [58]. Two pyrolysis chars were produced: (1) c. UWP (only from UWP), and (2) c. FW/CFS (from a mixture of 50 wt% FW and 50 wt% CFS). The char yields were 22 wt% for c. UWP, and 23 wt% for c. FW/CFS. Due to the internal diameter of the tar cracking reactor, chars were sieved to particle size varying from 0.5 to 1.6 mm to avoid edge-effects. To modify the physicochemical properties of the chars and in an attempt to improve their tar cracking efficiency, two chemical-free modification processes were applied: oxygenation by gas-phase treatment, and steam activation.

2.1.2. Oxygenation of the pyrolysis chars by O₂/N₂ gas-phase treatment

To increase the amount of oxygenated groups on the char surface, an O₂/N₂ gas-phase treatment was applied to the two pyrolysis chars. The dry chars were loaded in a vertical fixed-bed quartz reactor (bed height of 15 cm, internal diameter of 2.4 cm) and heated at 20 °C/min under pure nitrogen flow up to the oxygenation temperature (280 °C). Then, the nitrogen flow was replaced by a mixture of 8 v% O₂/92 v% N₂ at a flow rate of 2.0 L/min. Based on previous study [46], preliminary

tests were performed to determine the optimal conditions of oxygenation (temperature, duration). The pyrolysis chars were oxygenated at 280 °C during 4 h for c. UWP, and only 2 h for c. FW/CFS in order to limit the mass loss. Indeed, for modification processes, high solid yield is an important parameter in order to produce significant amount of catalyst from the available amount of char. Under the selected conditions, the solid yield of this treatment was 98 wt% for ox. UWP and 97 wt% for ox. FW/CFS, whereas after 4 h of oxygenation, the solid yield of ox. FW/CFS was only 57.4 wt%. The oxygenated chars were identified using the prefix “ox”.

2.1.3. Steam activation of the pyrolysis chars

A steam activation was applied to the two pyrolysis chars as this process is known to favour the development of micro, meso and macropores [59,60]. A 100 g sample of dry char was loaded in a semi-rotary quartz reactor (Carbolite HTR 11/150) and was heated to the activation temperature (850 °C) at a 10 °C/min heating rate in an inert atmosphere (N₂ flow rate of 0.5 L/min). At 850 °C, the activation started with the addition of steam (activating agent) to the nitrogen flow at a concentration of 15 v% during 80 min. The cooling of the reactor took place under inert atmosphere in order to preserve the catalysts properties for further characterisations. The resulting activated chars were named with the prefix “ac”. The solid yield of the steam activation was 77 wt% for ac. UWP, and 69 wt% for ac. FW/CFS. Table S.1 lists the different materials used in this study.

2.2. Characterization of feedstock and chars

2.2.1. Elemental composition

First, the moisture of the samples was eliminated with a drying step (105 °C in a furnace). The elemental composition (C, H, N, S) of the samples was determined with a Thermo Finnigan AE1112 Series Flash. The ash content of the chars was determined by measuring the residual mass after the combustion of 7.0 g of the sample for 15 h in a muffle furnace (Nabertherm P330) at 650 °C.

2.2.2. Mineral species

The chemical composition of the resulting ash was analysed by X-ray fluorescence spectroscopy (SHIMADZU EDX-800HS). Contrary to ICP-MS, the XRF method allows determining the chemical composition of a large sample (about 2 g against 20 mg with ICP-MS). The

analyses were performed under vacuum using powdered samples, with an acquisition time of 100 s. The ash was obtained from the combustion of around 20 g of each material. This significant amount of ash was used to analyse a sample representative of the materials.

The surfaces of the chars were observed by scanning electron microscopy (SEM) using a ZEISS DSM982 microscope equipped with a high-resolution Gemini column, operated at 10–15 kV. The local chemical composition at micro-scale was assessed by energy dispersive X-ray spectroscopy (EDX) using a Noran Voyager IV microanalysis system. For each char, several zones were analysed in order to obtain a statistical dataset representative of the materials.

2.2.3. O-functional groups

TPD analysis (coupled with μ -GC) was performed to quantify the O-functional groups on the char surface. The decomposition of O-containing groups occurs at a given temperature and is accompanied by a release of CO or CO₂ [46,61]. A 150 mg sample of char was introduced in a thermogravimetric analyser (Labsys T6 Evo) and flushed during 20 min under a pure nitrogen flow. The char was then heated from 30 to 1100 °C in an inert atmosphere (N₂ flow rate of 33 mL/min) with a heating rate of 5 °C/min. The gas produced (CO and CO₂) was analysed online with a μ -GC (My-GC, Agilent). Although the assignment of the peaks during TPD analysis is still discussed in the literature, global trends have emerged in previous studies [46,61]. The correlations are given in Table S.2. The deconvolution of the experimental data, performed with Matlab®, was used to quantify the amount of CO or CO₂ released for each desorption peak. Thus, the different O-containing groups can be identified and quantified.

2.2.4. Nature of the carbonaceous matrix

Raman spectroscopy was used to determine the different carbon structures of the chars. Raman spectra were acquired for each sample at room temperature and in air using a Confocal Raman – AFM WITTEC Alpha 300 AR microscope equipped with a CCD camera detector. Spectra were recorded using a 50 × lens (Na = 0.75) and an excitation laser at 532 nm in the 175-4000 cm⁻¹ Raman shift region. For each sample, at least two areas of 25 μ m² of three different particles were analysed. For ash-rich materials, a post treatment was applied to discriminate the mineral and the carbonaceous contributions. Then, the carbonaceous matrix was analysed according to a deconvolution method described elsewhere [62].

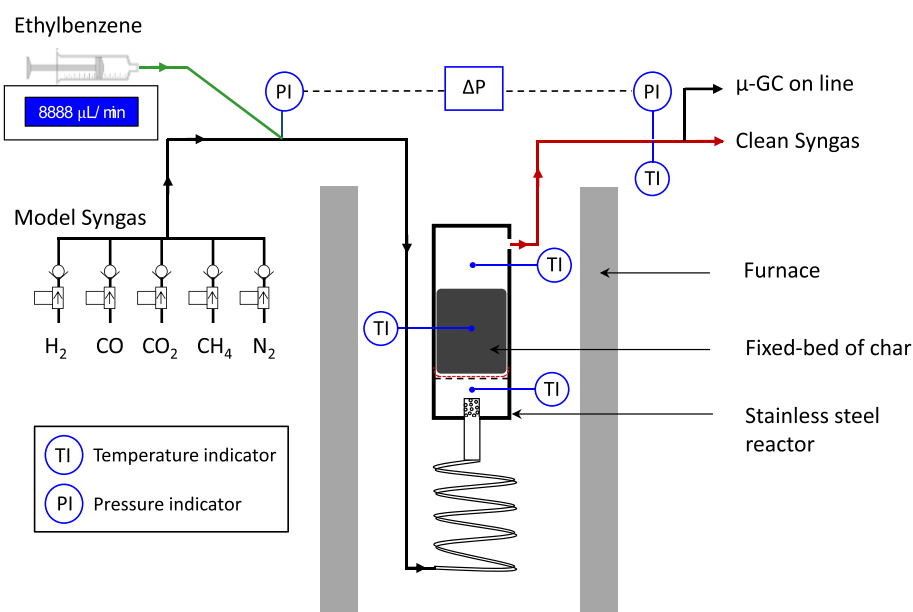


Fig. 1. Scheme of the device used for the tests of ethylbenzene decomposition.

2.2.5. Textural properties

The specific surface area, the pore size distribution and volume of the chars were studied by means of nitrogen adsorption-desorption at 77 K using a Micromeritics 3Flex apparatus. Prior to each measurement, the samples were outgassed under vacuum (1–30 μm Hg) at 30 °C during at least 16 h. The specific surface area was determined using the BET method, while the HK (Horvath-Kawazoe) and BJH (Barrett, Joyner, Halenda) methods were used to characterise the microporosity and mesoporosity, respectively. Textural properties of each sample were studied by at least three nitrogen adsorption-desorption isotherms.

2.3. Catalytic tests

2.3.1. Ethylbenzene cracking reactor

Ethylbenzene was chosen as tar surrogate and the catalytic cracking tests were carried out in a stainless-steel reactor (internal diameter 2.4 cm) placed in an electric furnace in which the heating was monitored by three thermocouples (Fig. 1).

The model syngas composition and flow rate were controlled by mass flow controllers connected to individual gas cylinders with a purity of 99.995%. Ethylbenzene was introduced in the gas flow by a syringe pump. The cracking tests were performed with an ethylbenzene concentration of 40 g/Nm³ representative to the tar concentrations in real syngas (5–200 g/Nm³) [2]. The mixture flowed in a preheater placed in the electric furnace, and entered on the bottom of the reactor. The exhaust gas was analysed online with a μ-GC (R-3000, SRA Instruments) and tar cracking products were identified using GC-MS (GC-MS Perkin Elmer Auto System XL). Details on the nature of the chromatographic columns and the analysis parameters are given on Table S.3.

The catalytic tests were performed at 650 °C, corresponding to a conventional syngas temperature at the gasifier outlet [1]. In these conditions, no supplementary heat source would be required to heat the syngas in the tar cracking process.

In an empty reactor set at 650 °C, the ethylbenzene conversion due to homogeneous reactions in a model syngas matrix (composed of H₂ (30%), CO (40%), CO₂ (15%) and N₂ (15%)) reached 68.4%. This conversion can also be explained by the catalytic activity of the stainless-steel reactor. To reduce the homogeneous cracking reactions, a less reactive gas composition was selected: CO (40 v%) and N₂ (60 v%). Thus, this gas matrix permitted to quantify the amount of permanent

gases (H₂, CO₂ ...) produced by the tar cracking reactions, and to evaluate the catalytic effect of the chars based on the ethylbenzene conversion. The bed height was 4.5 cm for all chars. Since the gas velocity was kept constant (9.6 cm/s), the residence time of the gas in empty column was 0.47 s at 650 °C. The degradation of the closure system of this reactor did not allow measuring precisely the bed weight evolution.

2.3.2. Experimental data evaluation

During the tar cracking reactions, the volumetric flow rate at the reactor outlet could vary. Thus, the nitrogen initially present in the model syngas was used as an internal standard, allowing the calculation of the real output volumetric flow rate of syngas.

The average ethylbenzene conversion (X_{EB}) was defined as the molar difference of ethylbenzene leaving the reactor (n_{EB}^{out}) to the ethylbenzene amount fed into the reactor (n_{EB}^{in}) over a given time, according to Eq. (1).

$$X_{EB} = \frac{n_{EB}^{in} - n_{EB}^{out}}{n_{EB}^{in}} \cdot 100 \quad (1)$$

The composition of the tar cracking products (named i) was discussed based on the molar selectivity (Sel_i), calculated with Eq. (2):

$$Sel_i = \frac{n_{prod,i}^{out}}{\sum n_{prod}^{out}} \cdot 100 \quad (2)$$

where $n_{prod,i}^{out}$ is the molar amount of the tar cracking product i at the reactor outlet.

The catalytic effect of the chars on ethylbenzene cracking was also evaluated through the atomic balances in carbon (η_C), reflecting the percentage of C atoms entering in the catalytic system that were in vapour phase at the reactor outlet.

$$\eta_C = \frac{n_C^{out}}{n_C^{in}} \cdot 100 \quad (3)$$

where:

- n_C^{in} is the amount of carbon atoms entering in the reactor,
- n_C^{out} is the amount of carbon atoms in the vapour phase at the reactor outlet.

Table 1
Solid yield, elemental analysis, and ash composition of the chars.

Solid yield (wt.%)	c.UWP	ox.UWP	ac.UWP	c.FW/CFS	ox.FW/CFS	ac.FW/CFS
		22.0	98.3	76.7	23.0	96.8
Elemental analysis (wt%)						
C	87.2 ± 1.0	84.3 ± 0.4	87.4 ± 1.7	44.1 ± 1.6	42.2 ± 1.6	32.6 ± 3.1
H	1.8 ± 0.2	1.8 ± 0.0	0.8 ± 0.1	1.3 ± 0.2	1.1 ± 0.0	0.9 ± 0.0
N	0.6 ± 0.2	0.7 ± 0.0	0.4 ± 0.0	3.1 ± 0.1	2.9 ± 0.1	1.4 ± 0.1
S	bdl	bdl	bdl	bdl	bdl	bdl
O (by difference)	8.3	9.7	8.9	4.5	7.8	5.7
Ash	2.1 ± 0.1	3.5 ± 0.4	2.5 ± 0.2	47.0 ± 0.0	45.9 ± 1.0	59.4 ± 3.4
Ash composition (wt.%)						
CaO	42.5	44.6	42.2	39.2	42.5	34.3
P ₂ O ₅	4.7	5.0	4.2	26.2	19.9	26.2
K ₂ O	11.0	12.9	13.2	6.4	6.7	7.2
Al ₂ O ₃	3.0	4.3	2.0	13.8	14.3	18.2
Cl	n.m	3.3	n.m	7.5	9.5	9.2
Fe ₂ O ₃	6.5	4.6	3.6	1.6	0.8	0.6
SO ₃	6.6	4.0	6.7	2.7	1.6	1.3
SiO ₂	8.0	6.8	4.4	2.0	1.8	2.2
MgO	11.0	8.4	13.4	n.m	2.1	n.m
Others (TiO ₂ , MnO, ZnO, CuO, SrO ...)	6.7	6.1	10.3	0.6	0.8	0.8

bdl: below the detection limit (< 0.2 wt%); n.m: non-measured (< 0.001 wt%).

3. Results and discussion

3.1. Effect of the modification process on the physicochemical properties of the chars

3.1.1. Chemical differences between UWP- and FW/CFS-based chars

Due to the different chemical composition of the initial wastes [62], two types of chars were obtained: chars from UWP were carbonaceous materials having carbon content higher than 84 wt%, while chars from FW/CFS were hybrid carbon/mineral materials (Table 1). Indeed, the materials obtained from FW/CFS presented a relatively low carbon content (32.6–44.1 wt%) counterbalanced by an important ash content (> 45.9 wt%). The composition of the ash is presented in Table 1 and was discussed in a previous communication [62].

The presence of small particles of calcium (0.5–5 μm) well distributed on the surface of FW/CFS-based chars was highlighted by the SEM observations, as shown in a previous study [62] and in Figure S.1.

The minerals speciation was characterised with Raman spectroscopy. A post treatment was applied to the Raman spectra obtained with FW/CFS-based chars in view to separate the mineral and the carbonaceous contributions, as described in a previous article [62]. Based on the RRUF database [63], the mineral contribution of FW/CFS Raman spectra was identified as hydroxyapatite (Ca₁₀(PO₄)₆(OH)₂). The chemical structure of the hydroxyapatite was confirmed by XRD analyses (Figure S.2).

The following paragraphs describe the physicochemical changes of the chars occurring during the modification processes.

3.1.2. Influence of the oxygenation process

It can be noticed from Table 1 that the oxygenation step did not significantly modified the elemental composition of the carbonaceous char (ox.UWP), while it slightly increased the oxygen content of the char rich in mineral species (ox.FW/CFS) from 4.5 to 7.8 wt%. However, as the oxygen content was calculated by difference, the values must be considered carefully.

Raman spectrum of the carbonaceous matrix of each char was analysed after a deconvolution treatment. The composition of the carbonaceous matrix is presented in Fig. 2. For ox. UWP and ox. FW/CFS, the oxygenation increased the proportion graphene-like sheets structures (+4.5 and + 2%, respectively) and reduced the defects in graphene-like sheets (−0.4% and −3.1%, respectively).

The precise catalytic role of O-functional groups on tar cracking reactions is not clear. These groups can interact with tar through

Table 2

Analysis of the O-functional groups present on the char surface using TPD-μ-GC technique.

Chars	Total amount	Basic Groups	Acidic groups
	(mmol/g)	(mol%)	(mol%)
c.UWP	0.28	39.8	60.2
ox.UWP	0.38	28.7	71.3
ac.UWP	0.16	59.1	40.9
c.FW/CFS	2.20	68.3	31.7
ox.FW/CFS	0.45	72.2	27.8
ac.FW/CFS	0.39	87.8	12.2

hydrogen bonds [11] or π – π^* stacking interactions promoting the multilayer adsorption of tar [64]. However, O-functional groups are thermally unstable and can be decomposed. This decomposition leads to the formation of free carbon sites on the char matrix that can catalyse the tar cracking reactions [65].

The Temperature Programmed Desorption analyses (Table 2) revealed the spectacular difference in the amount of O-functional groups between c. FW/CFS (2.2 mmol/g) and the other chars (< 0.45 mmol/g). While the oxygen content of ox. FW/CFS was higher than that of c. FW/CFS (7.8 and 4.5 wt%, respectively) (Table 1), the amount of O-functional groups was 4.9 times lower for ox. FW/CFS after the oxygenation. These results showed that the oxygenation step did not produce O-functional groups at the carbonaceous surface, but mainly oxidised the inorganic species of ox. FW/CFS, initially in metallic form due to the reductive atmosphere of the pyrolysis. Simultaneously, oxidation reactions of the carbonaceous matrix occurred during the oxygenation step resulting in the destruction of O-functional groups from the ox. FW/CFS surface (Table 2), and in the decrease of the graphene-like sheets structures containing defects (Fig. 2). The composition of O-functional groups is presented in Table S.4.

The effect of the oxygenation process on the textural properties of the chars was discussed in a previous article [66]. Whatever the chemical nature of the pyrolysis char, the specific surface area was not significantly modified by the oxygenation process. Both pyrolysis and oxygenated chars presented low porosity, with S_{BET} lower than 10 m²/g for FW/CFS-based chars, and lower than 80 m²/g for UWP-based chars [66].

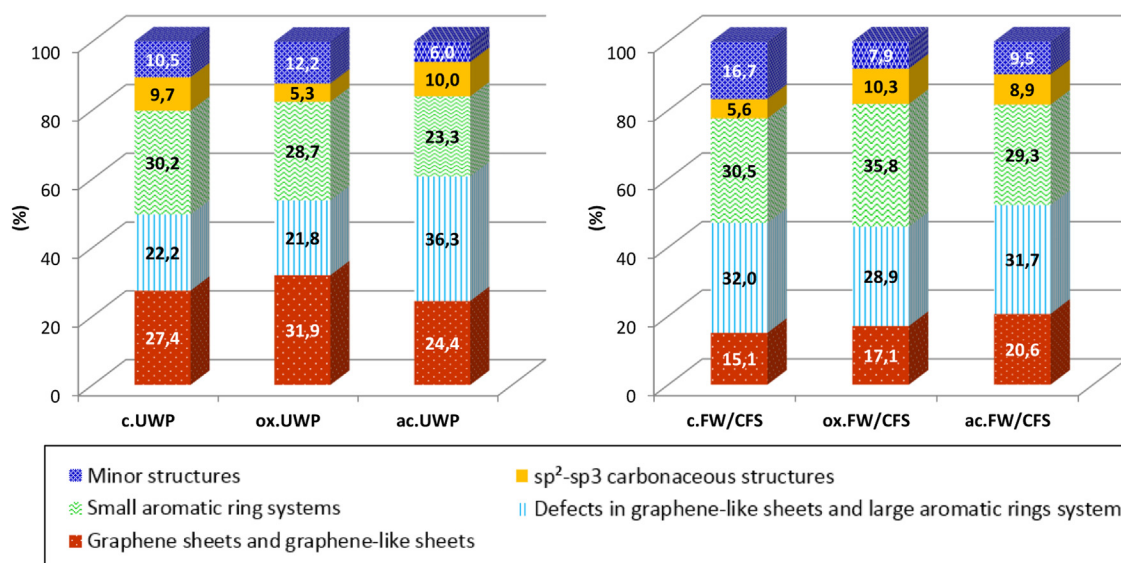


Fig. 2. Composition of the carbonaceous matrix of the chars determined with a deconvolution method of Raman spectra.

3.1.3. Influence of the steam activation process

The chemical composition of ac. UWP was not drastically modified by steam activation at 850 °C (Table 1). On the contrary, activation increased the ac. FW/CFS ash content (relative increase of 12.4 wt%) and decreased its carbon content (relative drop of 11.5 wt%). These evolutions resulted from the catalytic effect of the mineral species of c. FW/CFS on the gasification reactions of the carbonaceous matrix occurring during the activation step [67].

The effect of steam activation on the O-functional groups was similar for both types of chars (FW/CFS and UWP) (Table 2). Indeed, steam activation reduced the amount of O-functional groups, but raised the proportion of basic O-functional groups (+19%). The higher thermal stability of basic groups was mainly responsible for this evolution (Table S.2), as acidic groups were decomposed during the steam activation at 850 °C.

Contrary to oxygenation, steam activation strongly developed the specific surface area (S_{BET}) of the chars [66]. Microporous and mesoporous volumes were both increased by this process, which is in line with the literature results [59]. The S_{BET} of ac. UWP (625 m²/g) was more intensively developed than that of ac. FW/CFS (221 m²/g) during steam activation due to its superior carbon content (87.4 vs 32.6 wt%, respectively).

Steam activation also modified the carbonaceous matrix of the chars. Contrary to oxygenation, defects in graphene-like sheets (such as vacancy, Stone-Wales defects) significantly increased after steam activation, especially for ac. UWP (+14.5%). This evolution is explained by the interactions between the O atoms of steam and the carbonaceous matrix of the char.

The catalytic activity of these materials in ethylbenzene cracking reaction was studied in the following sections.

3.2. Effect of tar cracking over chars on the syngas production

3.2.1. Ethylbenzene conversion

The ethylbenzene conversion versus time of experiment for the different catalysts and for thermal cracking are presented in Fig. 3. For thermal cracking tests, the conversion of EB was initially 100% due to the catalytic activity of the stainless-steel reactor walls, and decays with time due to the deposition of non-active coke on the walls. Compared to thermal cracking, each char improved the ethylbenzene conversion. While ox. UWP, c. UWP and ox. FW/CFS were rapidly deactivated, three catalysts had higher catalytic activity but different catalytic behaviour: ac. FW/CFS, ac. UWP, and c. FW/CFS. During the first 30 min, the initial catalytic activity of c. FW/CFS and ac. UWP was similar and higher than that of ac. FW/CFS. Between 30 and 60 min, ac. FW/CFS was the most active catalyst while c. FW/CFS was more efficient than ac. UWP. For test duration longer than 60 min, the two activated chars (ac.FW/CFS and ac/UWP) remained substantially more efficient than the pyrolysis char c. FW/CFS.

The char ox. UWP was the less reactive catalyst and was completely deactivated after 85 min of reaction. Thus, the average conversion of ethylbenzene (X_{EB}) achieved within 85 min was calculated and the results are presented in Fig. 4. The horizontal line shows the result obtained from the non-catalytic thermal cracking test, with an average conversion of 37.2%. Two repetitions were performed with ac. UWP ($X_{\text{EB}} = 77.3\%$) and ac. FW/CFS ($X_{\text{EB}} = 85.8\%$) and the relative deviation was lower than 8% for ac. UWP, and lower than 2% for ac. FW/CFS, which was acceptable, as previously shown in the literature [68]. This deviation can be explained by the heterogeneity of waste-based chars, and by the catalytic contribution of the stainless-steel walls of the reactor.

The results revealed the antagonist effect of the two modification processes on the char activity. On the one hand, the oxygenation step negatively affected the catalytic activity of both chars, as reflected by the drastic drop of ethylbenzene conversion (from 53.2 to 41.3% for ox. UWP, and from 77.2 to 48.9% for ox. FW/CFS). On the other hand, the

steam activation significantly improved the catalytic performances of the chars. The ethylbenzene conversion reached 77.3% with ac. UWP, and 85.8% with ac. FW/CFS. It can be noticed that for similar conditions of production, the FW/CFS-based chars reached higher ethylbenzene conversion than UWP-based chars.

Within 85 min, the pyrolysis char c. FW/CFS appeared as an attractive catalyst due to its significant catalytic activity without the need for additional steam activation. However, above this time, the catalytic performance of c. FW/CFS decreased drastically compared to the activated chars (Fig. 3). After 170 min of test, the average ethylbenzene conversion was 57.0% for c. FW/CFS, 65.4% for ac. UWP, and 78.5% for ac. FW/CFS.

The effect of the catalytic activity of the chars on the composition of the produced gas was studied by investigating the reaction products selectivity.

3.2.2. Selectivity of the reaction products

Ethylbenzene (C₈H₁₀) was mostly decomposed to six molecules (Table 3): hydrogen (H₂), carbon dioxide (CO₂), styrene (C₈H₈), ethylene (C₂H₄), benzene (C₆H₆), and toluene (C₇H₈). It can be noticed that the carbon monoxide (CO) balance was slightly negative in all tests (except for ox. UWP), i.e. that the quantity consumed was higher than the quantity produced (Table S.5). This can be due to: (1) the reaction of CO with metal species of the char to form various types of carbonyls [69]; (2) the CO oxidation with the O-containing groups on the char surface producing CO₂, or (3) the Boudouard reaction (R6 in the next discussion). Indeed, the Boudouard reaction consumes CO to form CO₂ and C at temperature lower than 700 °C [70].

Based on the literature data dealing with ethylbenzene pyrolysis and tar cracking reactions, a set of reactions expected to be involved in the ethylbenzene decomposition has been identified. The styrene can be generated by the cracking reaction (R1) and the oxidative dehydrogenation of ethylbenzene “ODH” (R2) [71,72]. The ethylbenzene cracking reactions could also produce a wide range of molecules, such as toluene, benzene, ethylene, carbon dioxide or coke [73,74]. Although the experimental device did not allow a precise quantification of the bed weight evolution, coke formation was clearly observed.

The oxidative dehydrogenation of ethylbenzene (R2) also generates hydrogen. Hydrogen can then react with ethylbenzene through hydrogenolysis reactions (R3, R4), producing toluene and benzene [75]. Methane (CH₄) is produced by hydrogenolysis reactions, but it was not detected as an ethylbenzene cracking product in this study. This could result from its reaction with carbon dioxide by dry reforming reaction (R5), and/or by methane cracking reaction. Indeed, these reactions can

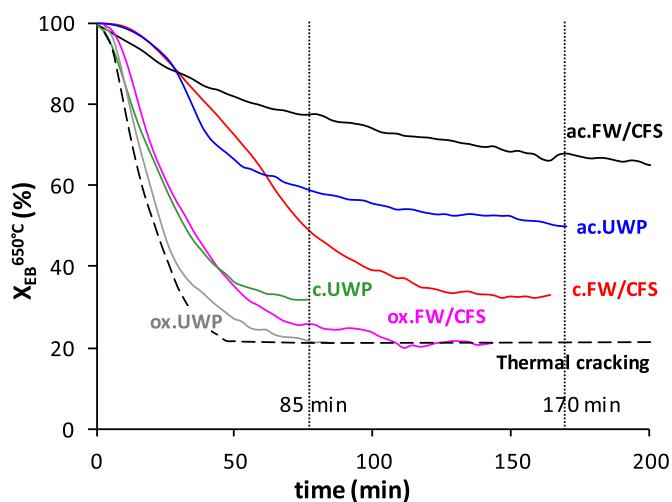


Fig. 3. Ethylbenzene conversion obtained with the different chars and during thermal cracking.

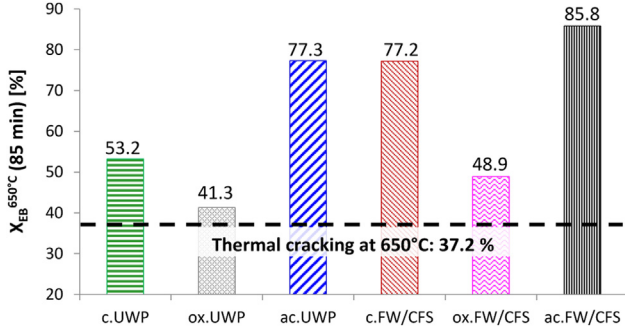


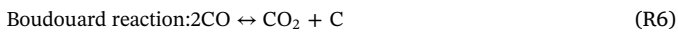
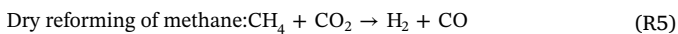
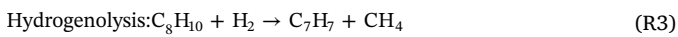
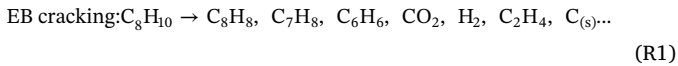
Fig. 4. Average conversion of ethylbenzene achieved with the different chars at 650 °C within 85 min of reaction (gas matrix: CO: 40%, N₂: 60%, EB: 40 g/Nm³).

Table 3

Molar selectivity of the products formed during the ethylbenzene cracking over the different chars and during thermal cracking within 85 min of test.

Materials	Selectivity of EB cracking products (mol%)					
	H ₂	CO ₂	C ₂ H ₄	C ₆ H ₆	C ₇ H ₈	C ₈ H ₈
Thermal cracking	34.4	14.8	7.6	0.0	1.4	41.8
c.UWP	41.7	20.3	3.5	5.1	2.2	27.2
ox.UWP	40.6	19.5	3.2	0.0	1.5	35.2
ac.UWP	52.3	13.4	1.7	3.6	2.8	26.2
c.FW/CFS	53.8	23.0	3.6	4.3	1.5	13.8
ox.FW/CFS	40.3	15.6	3.6	0.0	1.1	39.4
ac.FW/CFS	46.3	13.1	1.0	2.1	1.3	36.2

occur in the experimental conditions since they are initiated at 640 and 557 °C, respectively [76]. These reactions could also contribute to the coke production observed in our study. Ethylene was detected as an ethylbenzene cracking product and can be formed by aromatic ring-opening reactions from ethylbenzene, styrene, toluene, or benzene.



The catalytic effect of the chars was also discussed based on the carbon balance, reflecting the percentage of C atoms entering in the catalytic system that were in vapour phase at the reactor outlet. The atomic balance of carbon ranged between 85.2 and 98.9% (Table 4), confirming that ethylbenzene was catalytically decomposed and not adsorbed on the char surface.

Assuming that the lack of carbon at the reactor outlet is explained by the production of solid coke by ethylbenzene cracking reactions, and assuming this solid coke is pure carbon, the coke production over the 85 min of test (Coke_{prod}) was estimated according to the Eq. (4):

$$\text{Coke}_{\text{prod}} = n_{\text{C}}^{\text{in}} \left(1 - \frac{\eta_{\text{C}}}{100}\right) * M_{\text{C}} * 1000 \quad (4)$$

where:

- Coke_{prod} is the weight of coke theoretically produced (mg of coke/85 min of test),
- n_Cⁱⁿ is the amount of carbon atoms entering in the reactor (mol/

85 min of test),

- η_C is the atomic balance in carbon defined by Eq.(3),
- M_C is the molecular weight of carbon (12 g/mol).

The results evidenced that pyrolysis chars generated significant amount of coke, compared to other materials (Table 4). Indeed, the maximum theoretical coke production was obtained with c. FW/CFS and reached 2447 mg over the 85 min of test. Moreover, the coke production was almost similar for c. UWP and ac. UWP (1298 and 1174 mg, respectively), while the ethylbenzene conversion was significantly lower for c. UWP (53.2 vs 77.3%). This result confirms that the reactions promoted by the pyrolysis chars generated higher amount of coke. In addition, the evolutions of CO presented in Table S.5 revealed that the CO consumption was higher with the pyrolysis chars: -5.48% with c. FW/CFS, and -3.16% with c. UWP. All these results revealed that the catalytic activity of pyrolysis chars promoted the Boudouard reaction, leading to CO consumption and production of CO₂ and coke.

The objective of tar cracking consists in converting tar molecules into permanent gases in order to increase the syngas yield in a pyrogasification process. However, Table 3 showed that ethylbenzene was also decomposed into other tar molecules such as styrene, and toluene. The conversion of ethylbenzene into these tarry by-products does not increase the syngas production. The next paragraph studies the efficiency of the chars in converting ethylbenzene into syngas.

3.2.3. Production of syngas from tar cracking reactions

In order to determine the performance of each char for increasing the syngas production and quality, three parameters were calculated. As benzene can be considered as an interesting molecule for syngas valorisation as fuel in gas engine, these three parameters were calculated both including and excluding benzene as a syngas product.

First, for 100 mol of ethylbenzene entering into the catalytic reactor, the volume of syngas produced by cracking reactions over each char (Prod_{syngas}) was determined (Eq. (5)). This latter takes into account both the ethylbenzene conversion of the chars presented in Fig. 4, and the selectivity in tar cracking products (Table 3).

$$\text{Prod}_{\text{syngas}} = X_{\text{EB}} * \left(1 - \left(\frac{\sum S_{\text{tar prod}}}{100}\right)\right) * V_m \quad (5)$$

where S_{tar prod} is the selectivity in tarry reaction products (including or excluding benzene), and V_m = 22.4 NL/mol is the molar volume of ideal gas.

The lower heating value of the syngas produced (LHV_{syngas}) was also calculated to assess the quality of the syngas produced by tar cracking reactions:

$$\text{LHV}_{\text{syngas}} = \frac{\sum S_j * \text{LHV}_j}{\sum S_j} \quad (6)$$

where j is a permanent gas (H₂, CO₂, C₂H₄, with or without C₆H₆), S_j is the molar selectivity in permanent gas, and LHV_j is the lower heating value of the gas j (in kJ/mol).

Table 4

Carbon balance during the ethylbenzene cracking tests at 650 °C.

Materials	η _C (mol%)	Coke _{prod} (mg/85 min of test)
Thermal cracking	97.3	453
c.UWP	92.1	1298
c.FW/CFS	85.2	2447
ox.UWP	98.9	175
ox.FW/CFS	95.1	809
ac.UWP	92.9	1174
ac.FW/CFS	97.0	491

Then, the energy transferred from tar to syngas by the conversion of ethylbenzene in permanent gases (ΔE_{syngas} , expressed in kJ) was calculated with Eq. (7):

$$\Delta E_{\text{syngas}} = \text{Prod}_{\text{syngas}} * \frac{\text{LHV}_{\text{syngas}}}{22.4} \quad (7)$$

Results are presented in Table 5. First, it can be noticed that including benzene as a syngas compound strongly contribute to increase of the $\text{LHV}_{\text{syngas}}$, and thus to ΔE_{syngas} . For example, the selectivity of benzene was only 4.3% with c. FW/CFS. Including benzene as a syngas compound increases the $\text{LHV}_{\text{syngas}}$ from 221 to 368 kJ/mol of syngas produced, resulting in an increase of 75% of the energy transferred from tar to syngas (from 10.1 to 17.8 MJ/100 mol of initial tar). In the following discussion, the values excluding benzene will be discussed as in many studies, benzene is considered as a tar compound.

After oxygenation, the catalytic effect of both types of char on syngas production drastically decreased, with a drop of 25% for ox. UWP, and 37% for ox. FW/CFS (Table 5). It is interesting to note that steam activation decreased the $\text{LHV}_{\text{syngas}}$ for both types of char (from 225 to 221 kJ/mol for UWP-based chars, and from 221 to 208 kJ/mol for FW/CFS-based chars) but increased the syngas production ($\text{Prod}_{\text{syngas}}$). This latter increased by 26% for UWP-based chars, and by 4% for FW/CFS-based chars.

Although the highest ethylbenzene conversion was obtained with ac. FW/CFS (85.8%) (Fig. 4), the most efficient material for transferring energy from tar to syngas by the conversion of ethylbenzene (ΔE_{syngas}) was c. FW/CFS (10.14 MJ/100 mol of tar in). While steam activation slightly reduced the efficiency of ac. FW/CFS (9.86 MJ/100 of tar in), this modification process had a beneficial impact on the catalytic activity of ac. UWP. The ΔE_{syngas} of ac. UWP increased by 26% after activation. However, for both types of char, the oxygenation process dramatically decreased the catalytic efficiency. After oxygenation, ΔE_{syngas} was decreased by 26% and 30% for ox. UWP and ox. FW/CFS, respectively.

These results proved that the value of tar conversion is not sufficient to precisely assess the catalytic efficiency of a material.

Based on the characterization performed, the relationships between the char properties and their catalytic efficiency is discussed in the following paragraph.

3.2.4. Catalytic activity related to physicochemical properties

The lower carbon balance was obtained with c. FW/CFS (85.2%), together with the higher selectivity in hydrogen (53.8 mol%) and carbon dioxide (23.0 mol%). Table S.5 demonstrates that the higher consumption of CO during the catalytic tests also occurred with c. FW/CFS. These results suggested that c. FW/CFS strongly catalysed the aromatic ring-opening reactions (producing H_2 and CO_2) resulting in the significant ΔE_{syngas} obtained with this char (Table 5). This catalytic activity was explained by the metallic form of the mineral species present on c. FW/CFS surface, due to the reductive atmosphere of the pyrolysis gas [17]. The calcium particles well distributed on the surface of c. FW/CFS, and the presence of hydroxyapatite particles were expected to increase the catalytic activity of this material [77,78]. The strong activity of reduced metallic sites for the above-mentioned reactions (especially the Boudouard reaction) was confirmed by the significant consumption of CO and the high selectivity in CO_2 obtained with the two pyrolysis char (c.UWP and c. FW/CFS).

The oxidation of the mineral species of FW/CFS-based chars during the modification process (oxygenation, or steam activation) strongly changed the catalytic behaviour of these materials. Indeed, the activity of ox. FW/CFS and ac. FW/CFS for aromatic ring-opening reactions and Boudouard reaction strongly decreased, as evidenced by the lower selectivity in H_2 and CO_2 . In addition, these modification processes increased the proportion of basic O-functional groups (Table 2 and Table S.4), resulting in the promotion of oxidative dehydrogenation (ODH) of ethylbenzene responsible for the increase in styrene selectivity

(Table 3). Indeed, basic groups, such as quinone, are known to have a catalytic activity for the ethylbenzene dehydrogenation reaction [71,79,80]. As basic groups decompose at temperature higher than 840 °C (Table S.2) [46], they were stable under the experimental conditions (650 °C) and were thus available to catalyse ODH reactions.

For UWP-based chars, the beneficial effect of the high specific surface area of ac. UWP (625 m²/g) after steam activation balanced the detrimental effect of the metallic sites oxidation. The drastic increase of ethylbenzene conversion with ac. UWP compared to c. UWP (from 53.2 to 77.3%) improved the energy transferred from tar to syngas (Table 5). This efficiency could also result from the higher proportion of defects in graphene-like sheets in the carbonaceous matrix (Fig. 2) which were demonstrated to play a catalytic role in tar cracking reactions [52,65,81,82].

While steam activation had a positive impact on the UWP-based char reactivity, the oxygenation step had a detrimental effect on the catalytic activity of both types of char, by oxidizing the mineral active sites and decreasing the defects in graphene-like structures.

4. Conclusions

This paper investigated the catalytic activity of waste-derived chars in the cracking of ethylbenzene as a model tar molecule (surrogate of the light aromatic compounds), and aimed at studying the influence of chemical-free modification processes (steam activation, or gas-phase oxygenation) on the catalytic performance of the chars. This article is in line with two main issues in the development of the pyrogasification process: optimizing syngas yield and quality; and finding new valorization routes for residual chars.

Two chars were produced by pyrolysis: (1) used wood pallets (UWP), and (2) a mixture of food waste (FW, 50 wt%) and coagulation-flocculation sludge (CFS, 50 wt%). Catalytic tests were performed at 650 °C with an ethylbenzene concentration of 40 g/Nm³. Within the first 85 min of test, the average ethylbenzene conversion was 37.2% without catalyst due to the catalytic activity of the reactor walls, and reached 41.3–85.8% by using the chars. The higher ethylbenzene conversions were reached with the activated chars ac. FW/CFS and ac. UWP. Cracking, oxidative dehydrogenation, and hydrogenolysis reactions were involved in the decomposition mechanism of ethylbenzene. The objective of tar cracking consists in converting tar into gaseous products to increase the syngas yield. However, ethylbenzene conversion generated gaseous products (hydrogen, carbon dioxide, and ethylene) but also two tarry molecules (styrene, benzene and toluene) and coke.

Table 5

Lower heating value ($\text{LHV}_{\text{syngas}}$), volume of syngas produced from the cracking of 100 mol of ethylbenzene fed into the reactor ($\text{Prod}_{\text{syngas}}$) over each char samples. ΔE_{syngas} represents the energy transferred from tar to syngas by tar cracking reactions. These parameters were calculated both including and excluding benzene as a syngas product.

Materials	$\text{LHV}_{\text{syngas}}$ (kJ/mol syngas produced)		$\text{Prod}_{\text{syngas}}$ (NL syngas produced/ 100 mol tar)		ΔE_{syngas} (kJ/100 mol of initial tar)	
	With C_6H_6	Free of C_6H_6	With C_6H_6	Free of C_6H_6	With C_6H_6	Free of C_6H_6
Thermal cracking	324	323	474	474	6851	6846
c.UWP	434	225	842	782	16,327	7833
c.FW/CFS	368	221	1081	1027	17,773	10,143
ox.UWP	223	223	586	586	5828	5824
ox.FW/CFS	244	244	652	652	7108	7104
ac.UWP	371	221	1041	987	17,226	9739
ac.FW/CFS	308	208	1100	1063	15,119	9856

In order to determine the efficiency of each char in increasing the syngas production and quality, three parameters were calculated: the volume of syngas produced by tar cracking reaction ($\text{Prod}_{\text{syngas}}$), the lower heating value of the produced syngas ($\text{LHV}_{\text{syngas}}$), and the energy transferred from tar to syngas during the ethylbenzene decomposition (ΔE_{syngas}).

Despite the lower ethylbenzene conversion obtained with c. FW/CFS compared to ac. FW/CFS (77.2 vs 85.8%, respectively), c. FW/CFS was the most efficient material to increase the syngas yield and quality. For 100 mol of initial ethylbenzene entering in the system, the maximum energy transferred from tar to syngas was 10.14 MJ with c. FW/CFS. The significant efficiency of this char was explained by its catalytic activity for aromatic-ring opening reactions, resulting from its high content of mineral species in the metallic form.

The oxygenation process drastically decreased the catalytic activity of both types of char, due to the oxidation of the mineral active sites and the decrease of the graphene-like structures containing defects. On the contrary, steam sactivation increased the catalytic activity of ac. UWP, owing to the significant increase in specific surface area, and to the high proportion of defects in graphene-like sheets in the carbonaceous matrix.

This study demonstrated that waste-based chars were promising catalysts to convert the lost energy contained in tar into useful syngas.

Acknowledgement

This research was funded by the ANR Carnot M.I.N.E.S. The authors acknowledge the assistance for experiments and analyses from IMT Atlantique (Yvan Gouriou, Eric Chevrel, François-Xavier Blanchet, Jérôme Martin), IMT Mines Albi (Nathalie Lyczko, Laurène Haurie, Sylvie Del-Confetto, Mickaël Ribeiro, Pierre Bertorelle and Denis Marty) and Mines ParisTech' (Alain Thorel, Anthony Chesnaud and Sarah Berhanu).

Appendix A. Supplementary data

Supplementary data related to this article can be found at <https://doi.org/10.1016/j.biombioe.2018.07.020>.

References

- U. Arena, Process and technological aspects of municipal solid waste gasification. A review, *Waste Manag.* 32 (2012) 625–639, <https://doi.org/10.1016/j.wasman.2011.09.025>.
- T.A. Milne, R. Evans, N. Abatzoglou, *Biomass Gasifier Tars: Their Nature, Formation and Conversion.*, National Renewable Energy Laboratory, (1998).
- L. Le Coq, A. Duga, Syngas treatment unit for small scale gasification-application to IC engine gas quality requirement, *J. Appl. Fluid Mech.* 5 (2012) 95–103.
- L. Burhenne, T. Aicher, Benzene removal over a fixed bed of wood char: the effect of pyrolysis temperature and activation with CO₂ on the char reactivity, *Fuel Process. Technol.* 127 (2014) 140–148, <https://doi.org/10.1016/j.fuproc.2014.05.034>.
- Z. Abu El-Rub, E.A. Bramer, G. Brem, Review of catalysts for tar elimination in biomass gasification processes, *Ind. Eng. Chem. Res.* 43 (2004) 6911–6919, <https://doi.org/10.1021/ie0498403>.
- L. Devi, K.J. Ptasiński, F.J.J.G. Janssen, Pretreated olivine as tar removal catalyst for biomass gasifiers: investigation using naphthalene as model biomass tar, *Fuel Process. Technol.* 86 (2005) 707–730, <https://doi.org/10.1016/j.fuproc.2004.07.001>.
- P.J. Woolcock, R.C. Brown, A review of cleaning technologies for biomass-derived syngas, *Biomass Bioenergy* 52 (2013) 54–84, <https://doi.org/10.1016/j.biombioe.2013.02.036>.
- M.L. Valderrama Rios, A.M. González, E.E.S. Lora, O.A. Almazán del Olmo, Reduction of tar generated during biomass gasification: a review, *Biomass Bioenergy* 108 (2018) 345–370, <https://doi.org/10.1016/j.biombioe.2017.12.002>.
- A. Villot, Y. Gonthier, E. Gonze, A. Bernis, S. Ravel, M. Grateau, J. Guillaudeau, Separation of particles from syngas at high-temperatures with an electrostatic precipitator, *Separ. Purif. Technol.* 92 (2012) 181–190, <https://doi.org/10.1016/j.seppur.2011.04.028>.
- S.A. Nair, A.J.M. Pemen, K. Yan, F.M. van Gompel, H.E.M. van Leuken, E.J.M. van Heesch, K.J. Ptasiński, A.A.H. Drinkenburg, Tar removal from biomass-derived fuel gas by pulsed corona discharges, *Fuel Process. Technol.* 84 (2003) 161–173, [https://doi.org/10.1016/S0378-3820\(03\)00053-5](https://doi.org/10.1016/S0378-3820(03)00053-5).
- Y. Shen, J. Wang, X. Ge, M. Chen, By-products recycling for syngas cleanup in biomass pyrolysis – an overview, *Renew. Sustain. Energy Rev.* 59 (2016) 1246–1268, <https://doi.org/10.1016/j.rser.2016.01.077>.
- Y. Shen, K. Yoshikawa, Recent progresses in catalytic tar elimination during biomass gasification or pyrolysis—a review, *Renew. Sustain. Energy Rev.* 21 (2013) 371–392, <https://doi.org/10.1016/j.rser.2012.12.062>.
- S. Mani, J.R. Kastner, A. Juneja, Catalytic decomposition of toluene using a biomass derived catalyst, *Fuel Process. Technol.* 114 (2013) 118–125, <https://doi.org/10.1016/j.fuproc.2013.03.015>.
- Z. Abu El-Rub, E.A. Bramer, G. Brem, Experimental comparison of biomass chars with other catalysts for tar reduction, *Fuel* 87 (2008) 2243–2252, <https://doi.org/10.1016/j.fuel.2008.01.004>.
- Y. Shen, P. Zhao, Q. Shao, D. Ma, F. Takahashi, K. Yoshikawa, In-situ catalytic conversion of tar using rice husk char-supported nickel-iron catalysts for biomass pyrolysis/gasification, *Appl. Catal. B Environ.* 152–153 (2014) 140–151, <https://doi.org/10.1016/j.apcatb.2014.01.032>.
- L. Devi, K.J. Ptasiński, F.J.J.G. Janssen, S.V.B. van Paasen, P.C.A. Bergman, J.H.A. Kiel, Catalytic decomposition of biomass tars: use of dolomite and untreated olivine, *Renew. Energy* 30 (2005) 565–587, <https://doi.org/10.1016/j.renene.2004.07.014>.
- G. Guan, G. Chen, Y. Kasai, E.W.C. Lim, X. Hao, M. Kaewpanha, A. Abuliti, C. Fushimi, A. Tsutsumi, Catalytic steam reforming of biomass tar over iron- or nickel-based catalyst supported on calcined scallop shell, *Appl. Catal. B Environ.* 115–116 (2012) 159–168, <https://doi.org/10.1016/j.apcatb.2011.12.009>.
- J.F. González, S. Román, G. Engo, J.M. Encinar, G. Martínez, Reduction of tars by dolomite cracking during two-stage gasification of olive cake, *Biomass Bioenergy* 35 (2011) 4324–4330, <https://doi.org/10.1016/j.biombioe.2011.08.001>.
- D.A. Constantinou, J.L.G. Fierro, A.M. Efstathiou, A comparative study of the steam reforming of phenol towards H₂ production over natural calcite, dolomite and olivine materials, *Appl. Catal. B Environ.* 95 (2010) 255–269, <https://doi.org/10.1016/j.apcatb.2010.01.003>.
- M.F. Tennant, D.W. Mazyck, Steam-pyrolysis activation of wood char for superior odorant removal, *Carbon* 41 (2003) 2195–2202, [https://doi.org/10.1016/S0008-6223\(03\)00211-2](https://doi.org/10.1016/S0008-6223(03)00211-2).
- J.N. Kuhn, Z. Zhao, L.G. Felix, R.B. Slimane, C.W. Choi, U.S. Ozkan, Olivine catalysts for methane- and tar-steam reforming, *Appl. Catal. B Environ.* 81 (2008) 14–26, <https://doi.org/10.1016/j.apcatb.2007.11.040>.
- M. Virginie, C. Courson, D. Niznansky, N. Chaoui, A. Kiennemann, Characterization and reactivity in toluene reforming of a Fe/olivine catalyst designed for gas cleanup in biomass gasification, *Appl. Catal. B Environ.* 101 (2010) 90–100, <https://doi.org/10.1016/j.apcatb.2010.09.011>.
- P.R. Buchireddy, R.M. Bricka, J. Rodriguez, W. Holmes, Biomass gasification: catalytic removal of tars over zeolites and nickel supported zeolites, *Energy Fuels* 24 (2010) 2707–2715, <https://doi.org/10.1021/ef901529d>.
- M. Azhar Uddin, H. Tsuda, S. Wu, E. Sasaoka, Catalytic decomposition of biomass tars with iron oxide catalysts, *Fuel* 87 (2008) 451–459, <https://doi.org/10.1016/j.fuel.2007.06.021>.
- D. Sutton, B. Kelleher, J.R. Ross, Review of literature on catalysts for biomass gasification, *Fuel Process. Technol.* 73 (2001) 155–173.
- J. Chen, M. Tamura, Y. Nakagawa, K. Okumura, K. Tomishige, Promoting effect of trace Pd on hydrocalcite-derived Ni/Mg/Al catalyst in oxidative steam reforming of biomass tar, *Appl. Catal. B Environ.* 179 (2015) 412–421, <https://doi.org/10.1016/j.apcatb.2015.05.042>.
- S.J. Juutilainen, P.A. Simell, A.O.I. Krause, Zirconia: selective oxidation catalyst for removal of tar and ammonia from biomass gasification gas, *Appl. Catal. B Environ.* 62 (2006) 86–92, <https://doi.org/10.1016/j.apcatb.2005.05.009>.
- S. Cheah, K.R. Gaston, Y.O. Parent, M.W. Jarvis, T.B. Vinzant, K.M. Smith, N.E. Thornburg, M.R. Nimlos, K.A. Magrini-Bair, Nickel cerium olivine catalyst for catalytic gasification of biomass, *Appl. Catal. B Environ.* 134–135 (2013) 34–45, <https://doi.org/10.1016/j.apcatb.2012.12.022>.
- D.A. Constantinou, M.C. Álvarez-Galván, J.L.G. Fierro, A.M. Efstathiou, Low-temperature conversion of phenol into CO, CO₂ and H₂ by steam reforming over La-containing supported Rh catalysts, *Appl. Catal. B Environ.* 117–118 (2012) 81–95, <https://doi.org/10.1016/j.apcatb.2012.01.005>.
- L. Wang, Y. Hisada, M. Koike, D. Li, H. Watanabe, Y. Nakagawa, K. Tomishige, Catalyst property of Co–Fe alloy particles in the steam reforming of biomass tar and toluene, *Appl. Catal. B Environ.* 121–122 (2012) 95–104, <https://doi.org/10.1016/j.apcatb.2012.03.025>.
- K. Raveendran, A. Ganesh, K.C. Khilar, Influence of mineral matter on biomass pyrolysis characteristics, *Fuel* 74 (1995) 1812–1822, [https://doi.org/10.1016/0016-2361\(95\)80013-8](https://doi.org/10.1016/0016-2361(95)80013-8).
- N.B. Klinghoffer, M.J. Castaldi, A. Nzihou, Influence of char composition and inorganics on catalytic activity of char from biomass gasification, *Fuel* 157 (2015) 37–47, <https://doi.org/10.1016/j.fuel.2015.04.036>.
- P.H. Blanco, C. Wu, J.A. Onwudili, P.T. Williams, Characterization and evaluation of Ni/SiO₂ catalysts for hydrogen production and tar reduction from catalytic steam pyrolysis-reforming of refuse derived fuel, *Appl. Catal. B Environ.* 134–135 (2013) 238–250, <https://doi.org/10.1016/j.apcatb.2013.01.016>.
- J. Park, Y. Lee, C. Ryu, Reduction of primary tar vapor from biomass by hot char particles in fixed bed gasification, *Biomass Bioenergy* 90 (2016) 114–121, <https://doi.org/10.1016/j.biombioe.2016.04.001>.
- D. Feng, Y. Zhao, Y. Zhang, Z. Zhang, L. Zhang, S. Sun, In-situ steam reforming of biomass tar over sawdust biochar in mild catalytic temperature, *Biomass Bioenergy* 107 (2017) 261–270, <https://doi.org/10.1016/j.biombioe.2017.10.007>.
- G.P. Assima, A. Paquet, J.-M. Lavoie, Utilization of MSW-derived Char for Catalytic Reforming of Tars and Light Hydrocarbons in the Primary Syngas Produced during Wood Chips and MSW-rdf Air Gasification, *Waste Biomass Valorization*, (2017), pp.

- 1–20, <https://doi.org/10.1007/s12649-017-0138-0>.
- [37] H. Liu, T. Chen, D. Chang, D. Chen, H. He, R.L. Frost, Catalytic cracking of tar derived from rice hull gasification over pyalygorskite-supported Fe and Ni, *J. Mol. Catal. Chem.* 363–364 (2012) 304–310, <https://doi.org/10.1016/j.molcata.2012.07.005>.
- [38] Z. Min, M. Asadullah, P. Yimsiri, S. Zhang, H. Wu, C.-Z. Li, Catalytic reforming of tar during gasification. Part I. Steam reforming of biomass tar using ilmenite as a catalyst, *Fuel* 90 (2011) 1847–1854, <https://doi.org/10.1016/j.fuel.2010.12.039>.
- [39] J. Feroso, F. Rubiera, D. Chen, Sorption enhanced catalytic steam gasification process: a direct route from lignocellulosic biomass to high purity hydrogen, *Energy Environ. Sci.* 5 (2012) 6358–6367, <https://doi.org/10.1039/C2EE02593K>.
- [40] Y. Zhang, S. Kajitani, M. Ashizawa, Y. Oki, Tar destruction and coke formation during rapid pyrolysis and gasification of biomass in a drop-tube furnace, *Fuel* 89 (2010) 302–309, <https://doi.org/10.1016/j.fuel.2009.08.045>.
- [41] S. Hosokai, K. Norinaga, T. Kimura, M. Nakano, C.-Z. Li, J. Hayashi, Reforming of volatiles from the biomass pyrolysis over charcoal in a sequence of coke deposition and steam gasification of coke, *Energy Fuels* 25 (2011) 5387–5393, <https://doi.org/10.1021/ef2003766>.
- [42] A.V. Bridgwater, Review of fast pyrolysis of biomass and product upgrading, *Biomass Bioenergy* 38 (2012) 68–94, <https://doi.org/10.1016/j.biombioe.2011.01.048>.
- [43] P. Gilbert, C. Ryu, V. Sharifi, J. Swithenbank, Tar reduction in pyrolysis vapours from biomass over a hot char bed, *Bioresour. Technol.* 100 (2009) 6045–6051, <https://doi.org/10.1016/j.biortech.2009.06.041>.
- [44] S. Liu, Y. Wang, R. Wu, X. Zeng, S. Gao, G. Xu, Fundamentals of catalytic tar removal over in situ and ex situ chars in two-stage gasification of coal, *Energy Fuels* 1 (2014) 58–66.
- [45] F.-J. Wang, S. Zhang, Z.-D. Chen, C. Liu, Y.-G. Wang, Tar reforming using char as catalyst during pyrolysis and gasification of Shengli brown coal, *J. Anal. Appl. Pyrolysis* 105 (2014) 269–275, <https://doi.org/10.1016/j.jaap.2013.11.013>.
- [46] M. Ducouso, E. Weiss-Hortala, A. Nzihou, M.J. Castaldi, Reactivity enhancement of gasification biochars for catalytic applications, *Fuel* 159 (2015) 491–499, <https://doi.org/10.1016/j.fuel.2015.06.100>.
- [47] P. Lu, Q. Huang, Y. Chi, J. Yan, Preparation of high catalytic activity biochar from biomass waste for tar conversion, *J. Anal. Appl. Pyrolysis* 127 (2017) 47–56, <https://doi.org/10.1016/j.jaap.2017.09.003>.
- [48] N.B. Klinghoffer, M.J. Castaldi, A. Nzihou, Catalytic properties and catalytic performance of char from biomass gasification, *Ind. Eng. Chem. Res.* 51 (2012) 13113–13122, <https://doi.org/10.1021/ie3014082>.
- [49] S. Zhang, Y. Song, Y.C. Song, Q. Yi, L. Dong, T.T. Li, L. Zhang, J. Feng, W.Y. Li, C.-Z. Li, An advanced biomass gasification technology with integrated catalytic hot gas cleaning. Part III: effects of inorganic species in char on the reforming of tars from wood and agricultural wastes, *Fuel* 183 (2016) 177–184, <https://doi.org/10.1016/j.fuel.2016.06.078>.
- [50] D.M. Keown, J.-I. Hayashi, C.-Z. Li, Drastic changes in biomass char structure and reactivity upon contact with steam, *Fuel* 87 (2008) 1127–1132, <https://doi.org/10.1016/j.fuel.2007.05.057>.
- [51] P. Fu, S. Hu, L. Sun, J. Xiang, T. Yang, A. Zhang, J. Zhang, Structural evolution of maize stalk/char particles during pyrolysis, *Bioresour. Technol.* 100 (2009) 4877–4883, <https://doi.org/10.1016/j.biortech.2009.05.009>.
- [52] Z. Min, P. Yimsiri, M. Asadullah, S. Zhang, C.-Z. Li, Catalytic reforming of tar during gasification. Part II. Char as a catalyst or as a catalyst support for tar reforming, *Fuel* 90 (2011) 2545–2552, <https://doi.org/10.1016/j.fuel.2011.03.027>.
- [53] G. Yildiz, F. Ronse, R. Venderbosch, R. van Duren, S.R.A. Kersten, W. Prins, Effect of biomass ash in catalytic fast pyrolysis of pine wood, *Appl. Catal. B Environ.* 168–169 (2015) 203–211, <https://doi.org/10.1016/j.apcatb.2014.12.044>.
- [54] O. Mašek, N. Sonoyama, E. Ohtsubo, S. Hosokai, C.-Z. Li, T. Chiba, J. Hayashi, Examination of catalytic roles of inherent metallic species in steam reforming of nascent volatiles from the rapid pyrolysis of a brown coal, *Fuel Process. Technol.* 88 (2007) 179–185, <https://doi.org/10.1016/j.fuproc.2006.03.004>.
- [55] T. Sueyasu, T. Oike, A. Mori, S. Kudo, K. Norinaga, J. Hayashi, Simultaneous steam reforming of tar and steam gasification of char from the pyrolysis of potassium-loaded woody biomass, *Energy Fuels* 26 (2012) 199–208, <https://doi.org/10.1021/ef201166a>.
- [56] D. Feng, Y. Zhao, Y. Zhang, S. Sun, S. Meng, Y. Guo, Y. Huang, Effects of K and Ca on reforming of model tar compounds with pyrolysis biochars under H₂O or CO₂, *Chem. Eng. J.* 306 (2016) 422–432, <https://doi.org/10.1016/j.cej.2016.07.065>.
- [57] P. Lu, X. Qian, Q. Huang, Y. Chi, J. Yan, Catalytic cracking of toluene as a tar model compound using sewage-sludge-derived char, *Energy Fuels* 30 (2016) 8327–8334, <https://doi.org/10.1021/acs.energyfuels.6b01832>.
- [58] E. Mura, O. Debono, A. Villot, F. Paviet, Pyrolysis of biomass in a semi-industrial scale reactor: study of the fuel-nitrogen oxidation during combustion of volatiles, *Biomass Bioenergy* 59 (2013) 187–194, <https://doi.org/10.1016/j.biombioe.2013.09.001>.
- [59] M. Molina-Sabio, M.T. Gonzalez, F. Rodriguez-Reinoso, A. Sepúlveda-Escribano, Effect of steam and carbon dioxide activation in the micropore size distribution of activated carbon, *Carbon* 34 (1996) 505–509, [https://doi.org/10.1016/0008-6223\(96\)00006-1](https://doi.org/10.1016/0008-6223(96)00006-1).
- [60] N. Mohamad Nor, L.C. Lau, K.T. Lee, A.R. Mohamed, Synthesis of activated carbon from lignocellulosic biomass and its applications in air pollution control—a review, *J. Environ. Chem. Eng.* 1 (2013) 658–666, <https://doi.org/10.1016/j.jece.2013.09.017>.
- [61] J.-H. Zhou, Z.-J. Sui, J. Zhu, P. Li, D. Chen, Y.-C. Dai, W.-K. Yuan, Characterization of surface oxygen complexes on carbon nanofibers by TPD, XPS and FT-IR, *Carbon* 45 (2007) 785–796, <https://doi.org/10.1016/j.carbon.2006.11.019>.
- [62] M. Hervy, S. Berhanu, E. Weiss-Hortala, A. Chesnaud, C. Gérente, A. Villot, D. Pham Minh, A. Thorel, L. Le Coq, A. Nzihou, Multi-scale characterisation of chars mineral species for tar cracking, *Fuel* 189 (2017) 88–97, <https://doi.org/10.1016/j.fuel.2016.10.089>.
- [63] R.T. Downs, The RRUFF Project: an Integrated Study of the Chemistry, Crystallography, Raman and Infrared Spectroscopy of minerals., Program Abstr. 19th Gen. Meet. Int. Mineral. Assoc. Kobe Jpn. O03–O13. (n.d.).
- [64] W.-J. Liu, F.-X. Zeng, H. Jiang, X.-S. Zhang, Preparation of high adsorption capacity bio-chars from waste biomass, *Bioresour. Technol.* 102 (2011) 8247–8252, <https://doi.org/10.1016/j.biortech.2011.06.014>.
- [65] A. Dufour, A. Celzard, V. Fierro, E. Martin, F. Broust, A. Zoulalian, Catalytic decomposition of methane over a wood char concurrently activated by a pyrolysis gas, *Appl. Catal. Gen.* 346 (2008) 164–173, <https://doi.org/10.1016/j.apcata.2008.05.023>.
- [66] M. Hervy, D. Pham Minh, C. Gérente, E. Weiss-Hortala, A. Nzihou, A. Villot, L. Le Coq, H₂S removal from syngas using wastes pyrolysis chars, *Chem. Eng. J.* 334 (2018) 2179–2189, <https://doi.org/10.1016/j.cej.2017.11.162>.
- [67] C. Dupont, S. Jacob, K.O. Marrakchy, C. Hognon, M. Grateau, F. Labalette, D. Da Silva Perez, How inorganic elements of biomass influence char steam gasification kinetics, *Energy* 109 (2016) 430–435, <https://doi.org/10.1016/j.energy.2016.04.094>.
- [68] F. Nestler, L. Burhenne, M.J. Amtenbrink, T. Aicher, Catalytic decomposition of biomass tars: the impact of wood char surface characteristics on the catalytic performance for naphthalene removal, *Fuel Process. Technol.* 145 (2016) 31–41, <https://doi.org/10.1016/j.fuproc.2016.01.020>.
- [69] U. Arena, F. Di Gregorio, Energy generation by air gasification of two industrial plastic wastes in a pilot scale fluidized bed reactor, *Energy* 68 (2014) 735–743, <https://doi.org/10.1016/j.energy.2014.01.084>.
- [70] P. Lahijani, Z.A. Zainal, M. Mohammadi, A.R. Mohamed, Conversion of the greenhouse gas CO₂ to the fuel gas CO via the Boudouard reaction: a review, *Renew. Sustain. Energy Rev.* 41 (2015) 615–632, <https://doi.org/10.1016/j.rser.2014.08.034>.
- [71] M.F.R. Pereira, J.J.M. Orfao, J.L. Figueiredo, Oxidative dehydrogenation of ethylbenzene on activated carbon catalysts. I. Influence of surface chemical groups, *Appl. Catal. Gen.* 184 (1999) 153–160.
- [72] S. Gomez Sanz, L. McMillan, J. McGregor, J.A. Zeitle, N. Al-Yassir, S. Al-Khattaf, L.F. Gladden, A new perspective on catalytic dehydrogenation of ethylbenzene: the influence of side-reactions on catalytic performance, *Catal Sci Technol* 5 (2015) 3782–3797, <https://doi.org/10.1039/C5CY00457H>.
- [73] Q. Chen, G.F. Froment, Thermal cracking of substituted aromatic hydrocarbons. II. Kinetic study of the thermal cracking of n-propylbenzene and ethylbenzene, *J. Anal. Appl. Pyrolysis* 21 (1991) 51–77, [https://doi.org/10.1016/0165-2370\(91\)80015-Z](https://doi.org/10.1016/0165-2370(91)80015-Z).
- [74] C. Hermann, P. Quicker, R. Dittmeyer, Mathematical simulation of catalytic dehydrogenation of ethylbenzene to styrene in a composite palladium membrane reactor, *J. Membr. Sci.* 136 (1997) 161–172, [https://doi.org/10.1016/S0376-7388\(97\)81990-4](https://doi.org/10.1016/S0376-7388(97)81990-4).
- [75] C. Hoang-Van, B.L. Villemin, S.J. Teichner, Hydrogenolysis of ethylbenzene over a supported nickel catalyst derived from nickel hydroaluminate, *J. Catal.* 105 (1987) 469–477, [https://doi.org/10.1016/0021-9517\(87\)90074-1](https://doi.org/10.1016/0021-9517(87)90074-1).
- [76] S. Wang, G.Q. Lu, G.J. Millar, Carbon dioxide reforming of methane to produce synthesis gas over metal-supported catalysts: state of the art, *Energy Fuels* 10 (1996) 896–904.
- [77] B. Rêgo De Vasconcelos, L. Zhao, P. Sharrock, A. Nzihou, D. Pham Minh, Catalytic transformation of carbon dioxide and methane into syngas over ruthenium and platinum supported hydroxyapatites, *Appl. Surf. Sci.* 390 (2016) 141–156, <https://doi.org/10.1016/j.apsusc.2016.08.077>.
- [78] T.S. Phan, A.R. Sane, B. Rêgo de Vasconcelos, A. Nzihou, P. Sharrock, D. Grouset, D. Pham Minh, Hydroxyapatite supported bimetallic cobalt and nickel catalysts for syngas production from dry reforming of methane, *Appl. Catal. B Environ.* 224 (2018) 310–321, <https://doi.org/10.1016/j.apcatb.2017.10.063>.
- [79] A. Schraut, G. Emig, H.-G. Sockel, Composition and structure of active coke in the oxydehydrogenation of ethylbenzene, *Appl. Catal., A* 29 (1987) 311–326, [https://doi.org/10.1016/S0166-9834\(00\)82901-2](https://doi.org/10.1016/S0166-9834(00)82901-2).
- [80] Y. Iwasawa, H. Nobe, S. Ogasawara, Reaction mechanism for styrene synthesis over polynaphthoquinone, *J. Catal.* 31 (1973) 444–449.
- [81] X. Li, C. Li, Volatilisation and catalytic effects of alkali and alkaline earth metallic species during the pyrolysis and gasification of Victorian brown coal. Part VIII. Catalysis and changes in char structure during gasification in steam, *Fuel* 85 (2006) 1518–1525, <https://doi.org/10.1016/j.fuel.2006.01.007>.
- [82] D.P. Serrano, J.A. Botas, J.L.G. Fierro, R. Guil-López, P. Pizarro, G. Gómez, Hydrogen production by methane decomposition: origin of the catalytic activity of carbon materials, *Fuel* 89 (2010) 1241–1248, <https://doi.org/10.1016/j.fuel.2009.11.030>.